

DESIGN IMPROVEMENTS IN LINERS FOR
GLASS-FIBER FILAMENT-WOUND TANKS
TO CONTAIN CRYOGENIC FLUIDS

Contract NAS 3-4189

Report No. 0889-01-1 (Quarterly)

Period Covered: 1 July to 30 September 1964

Prepared By

Aerojet-General Corporation
Structural Materials Division
Von Karman Center
Azusa, California

GPO PRICE \$ _____

OTS PRICE(S) \$ _____

Author: R. N. Hanson

Hard copy (HC) 3.00

Microfiche (MF) .50

October 1964

Prepared For

NASA, Lewis Research Center
Cleveland, Ohio

602 FORM 10-64

N 65 12622	(THRU)
ACCESSION NUMBER	(CODE)
56	33
(PAGES)	(CATEGORY)
02-59763	
NASA CR OR TXR OR AD NUMBER	

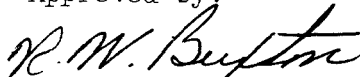
FOREWORD

This report was prepared by the Structural Materials Division of Aerojet-General Corporation, under NASA Contract Number NAS 3-4189, "Design Improvements in Liners for Glass Fiber Filament-Wound Tanks to Contain Cryogenic Fluids." The work on this contract is under the direction of the NASA-Lewis Research Center, Advanced Rocket Technology Branch, with Mr. James R. Barber as the A.R.T.B. Project Manager.


The report covers work conducted from 1 July 1964 through 30 September 1964, and is submitted in partial fulfillment of the contract.

The program was conducted by personnel from the Structural Engineering Department under F. J. Darms, Department Head. Those contributing to this report included R. W. Buxton, Program Manager; R. N. Hanson, Principal Investigator; and D. Fernandez and G. A. Lunde, Structural Analysis.

Approved by:


R. W. Buxton
Program Manager

Approved by:


F. J. Darms, Manager
Structural Engineering Dept.

CONTENTS

	<u>Page</u>
I. INTRODUCTION _____	1
II. PROGRAM PLAN _____	2
A. Task I Study _____	2
B. Task II - 18-in.-dia Specimens _____	4
III. DISCUSSION _____	4
A. Selection of Materials _____	4
B. Geometric Analysis _____	10
C. Series Number One Specimen Test _____	10
IV. ANTICIPATED WORK FOR NEXT PERIOD _____	11

References

	<u>Table</u>
Results of Uniaxial Tension Tests _____	1
	<u>Figure</u>
Summary of Planned Program _____	1
Pressure Required to Attain 0.025-in./in. Strain at Cryogenic Temperature vs Longitudinal Wrap Thickness _____	2
Uniaxial Tensile Specimen Testing _____	3
Polyurethane and Epoxy Foam Specimens after Compression Test in Liquid Nitrogen _____	4
Biaxial Strain Fixture in Instron Tensile Testing Machine _____	5
Fabrication and Test Procedure for Biaxial Strain Specimens _____	6
Liner Patterns to be Investigated _____	7
Sample Liner Patterns After Testing in Biaxial Strain Fixture _____	8

CONTENTS (cont.)

APPENDIX - GEOMETRIC ANALYSIS

	<u>Table</u>
Corrugation Geometry Variables _____	A-1
	<u>Figure</u>
Corrugation Analytical Model _____	A-1
Typical Corrugation - Pattern Length Definition _____	A-2

I. INTRODUCTION

The Structural Materials Division of the Aerojet-General Corporation was awarded Contract NAS 3-4189 from the NASA Lewis Research Center, Advanced Rocket Technology Branch, to develop design improvements in liners for glass-filament-wound tanks. The design improvements should enable the liner materials to tolerate the strains associated with the high fiber stresses typical of this type of pressure vessel. The purpose of the program is to increase the strain tolerance of polymeric film and metal foil liners by the incorporation of corrugations and pleats. Ultimate objectives of the program are to establish liner designs, for liquid-hydrogen tanks, that are capable of meeting repeated operating strains to 2.5% in all directions, while withstanding a maximum tank pressure of 175 psi.

The reason for the interest in filament-wound tankage is the high demonstrated performance of the composite structure. This performance, with its accompanying high operating fiber stresses and strains, introduces extremely difficult and, as yet, unresolved design problems when the liner, necessary for the containment of the cryogenic fluids, is considered. This is because no homogeneous impermeable material has been developed that can withstand repeated equal bidirectional strains to 2.5% at liquid-oxygen and liquid-nitrogen temperatures.

The principal problems that must be solved in this program are ones of design. These problems associated with the design of the corrugations are: the shape; the spacing; methods of providing equal strains in all directions (i.e., pattern geometry); compatibility with hard points; techniques to support the liner against buckling and shearing away from the composite wall; and adaptation, and integration, of liner and filament-winding process for maximum compatibility.

The program has been directed to resolve the design problems by the selection of materials of construction, the analysis of the geometric shape, spacing, and intersections, the performance of specimen tests using 8-in.-dia pressure vessels, and finally the fabrication and testing of three 18-in.-dia chambers. The analytical portion of the program has been limited to the analysis necessary for the selection of the designs for experimentation, and for the definition of geometries that provide the required strains within the elastic limit of the liner materials. It is not expected that the theoretical analysis will predict accurately the vessel performance because of areas of high local stress concentration which can reduce the cyclic life of the liner, but which are not readily predicted by analytical analysis. The program is thus concentrated on the empirical results obtained from specimen tests. Evaluation of preliminary designs will be made through the fabrication and test of 14 lined filament-wound tanks 8 in. in dia by 12-in. long. Based on these test data, a design, or designs, for three 18-in.-dia by 26-in. long filament-wound pressure vessels will be established. These chambers will be fabricated and cyclic tested to substantiate the design concepts.

II. PROGRAM PLAN

The schedule for this program, based on completion of the technical effort during a 12-month period, is presented in Figure 1. Two major areas of effort have been defined as Task I - Study and Task II - 18-in.-dia Specimens.

A. TASK I - STUDY

1. Materials Selection

This study has been established to categorize the physical and structural properties for the candidate liner materials:

- a. Type 304 stainless steel
- b. Aluminum alloy
- c. Mylar or metal foil laminated to Mylar
- d. Kel-F or metal foil laminated to Kel-F.

ABSTRACT

12622

A materials selection study has been conducted to establish material physical properties and evaluate them in terms of fabrication and design requirements. A geometric analysis has been made to develop equations which define liner stresses and which control pattern geometry.

The S and crossing patterns have been selected for evaluation in the first series of 8-in.-dia specimen tests based on results of the biaxial strain testing. Liners for the first series of test specimens will be fabricated from Type 304 stainless steel foil; 1100 aluminum foil; Mylar laminated to aluminum foil; and Kel-F laminated to aluminum foil. Both the S and crossing patterns will be fabricated from each of these materials for a total of 8 specimens. These specimens will be 8-in.-dia chambers fabricated with a Dacron-resin composite having 35% bosses and a length-to-diameter ratio of 1.4.

Author

Included are a review of physical properties in relation to the fabrication and design requirements of the pressure vessels, and an evaluation of specific pattern geometries by bi-axial tension testing.

2. Geometric Analysis

This study was established to provide a detailed structural analysis of the elements of the two basic corrugation arrangements (crossing and S-shaped). A parametric study will be made, on an IBM 7094 computer, to evaluate corrugation designs in terms of material, physical properties; internal pressure; liner thickness; depth of corrugations; radii of curvature; spacing; point of support; cross-sectional shape; and coefficient of thermal contraction of liner and case.

3. Specimen Tests

Three series of 8-in.-dia specimens tests will be made under this study to establish the design for the 8-in.-dia vessels.

a. Series No. 1

The designs for this series of eight specimens will be established from the studies performed under the selection of materials and geometric analysis. Two basic designs will be established for metal foil liners and two for polymer film liners. All specimens will be tested in liquid nitrogen.

b. Series No. 2

Two designs for test series No. 2 will be established based on test results of test series No. 1, modified as required. The selection will be based on operating strains and number of cycles obtained. A total of four 8-in.-dia specimens will be tested, two in LN_2 and two in LH_2 .

c. Series No. 3

A final design will be established based on series No. 2. One specimen each will be fabricated for testing in LN_2 and LH_2 .

B. TASK II - 18-IN.-DIA SPECIMENS

The 18-in.-dia by 26-in. long filament-wound tanks for the second task will be fabricated to the liner design (selected from Task I, with approval of the ARTB Project Manager) found to be best for application with liquid hydrogen. Processes and test techniques developed for the 8-in.-dia specimens of Task I will be used in processing these chambers. Two chambers will be cycled with LN_2 and one chamber cycled with LH_2 . These chambers will be cycled 100 times, or until failure occurs.

III. DISCUSSION

A. SELECTION OF MATERIALS

Two basic tasks were established under this study: establishment of the physical properties of the candidate materials for the composite, liners, and corrugation support; and evaluation of materials in terms of fabrication and design requirements.

1. Establish Physical Properties

a. Composite Structure

The maximum expected operating pressure for liquid oxygen or hydrogen tankage is approximately 175 psi. An efficient glass-fiber filament-wound tank would be operating at a strain level of approximately 2-1/2% at this pressure. Operating strains in the composite structure are a function of the chamber pressure, radius, thickness, and modulus. An analysis has been made to select a composite material which will permit operating strains of 2-1/2% in the small diameter specimens being fabricated under this program while still maintaining a realistic chamber pressure and composite wall-thickness. Figure 2 presents a plot of chamber pressure vs required longitudinal composite wall thickness for composite structures of both E-801 glass and Dacron. Curves are plotted for both 8 and 18-in.-dia vessels operating at 2.5% strain, based on material properties modified for cryogenic temperature (see References 1 and 2). The minimum practical longitudinal composite wall thickness is controlled by the fabrication process and is approximately 0.008-in. for the glass-resin composite and 0.015-in. for the Dacron-resin composite. As shown in Figure 2, the

minimum operating pressure for the glass-resin composite is 800 psi for the 8-in.-dia and 345 psi for the 18-in.-dia chambers. A chamber pressure of 175 psi can be obtained using a Dacron-resin composite in both the 8-in.-dia and 18-in.-dia specimens at composite wall thicknesses of 0.017 and 0.037-in., respectively.

Stresses developed in the liner support material are directly proportional to the chamber pressure. The amount and density of the support material is directly related to this stress. For this reason the first series of 8-in.-dia chambers will be fabricated with a Dacron-resin composite, thus allowing a realistic chamber pressure and minimization of support material.

b. Liner Materials

The basic physical properties of the candidate liner materials (Sections II,A,1) that must be established as required by the geometric analysis are: (1) yield strength, (2) modulus of elasticity, (3) coefficient of thermal expansion, and (4) permeability. These physical properties, with the exception of permeability, are established as a function of temperature for each of the candidate liner materials (Reference 3) down to -320°F . These data will be extrapolated down to -420°F , as required for design.

The permeability of the aluminum and stainless steel can be considered to be zero for specimen design. A survey was made for permeability data for the candidate liner materials Mylar and Kel-F (References 4 and 5). Permeability values reported were not consistent, with most values reported at room temperature. The variations appear to be the result of the test method. No further effort will be expended in this area for the following reasons: first, the liner materials of specific interest in the program are well defined by contract; and, second, the reported permeability data is of questionable value to the specific problem at cryogenic temperature.

Fabrication of sample liner geometries for testing in the biaxial strain fixture (discussed in Section III,A,2) revealed that the ultimate elongation of 60%, reported in Reference 3, for 304 stainless steel was not obtained during forming. Specimens which were formed from 1-mil Type 304 stainless steel ruptured at elongations of approximately 30%. The

elongation data reported in the literature were established from much thicker material sections. As the total elongation is a function of material thickness, tensile tests were run on the candidate liner materials to establish actual ultimate elongations. Standard tensile test specimens per ASTM E-861T were pulled for samples of: 6-, 8-, 12-, and 16-mil 1100 aluminum; 3- and 5-mil 304 stainless steel; and 3- and 6-mil 347 stainless steel. The test setup, and typical specimens before and after failure are shown in Figure 3. Results of these tests are shown in Table 1 as ultimate elongation and yield strength. Each data point is the average value of five tensile specimens. Ultimate elongations values for aluminum were 25% below reported data, while those for the stainless steels were 40% below. The trend of decreasing elongation with decreasing material thickness is clearly established.

c. Corrugation Support

As indicated by the analytical analysis (see Section III,B), some type of corrugation support material will be required to minimize the bending stresses in the liner material. Two types of foam have been tested to establish deflection and load relationships at cryogenic temperatures. A 2-lb/ft³ density epoxy foam, and polyurethane foams of 3-, 5-, and 9-lb/ft³ density were compression tested at -320°F. The test specimen was a right circular cylinder 2 in. in diameter and 4 in. high. The specimens were immersed in LN₂ and soaked for 30 min. A compression test was then run on the specimen while still submerged.

The 2-lb density epoxy foam was Magnolia Foam No. 1716, parts A and B, with a ratio of 11 to 1 by weight, respectively. Two specimens of this foam were tested. These specimens would develop their ultimate compressive stress, fail and relieve load, and repeat the process. Test values for deflection and ultimate load have been established at the first failure point.

<u>Specimen No.</u>	<u>Deflection, %</u>	<u>Compressive Strength, psi</u>	<u>Modulus, psi</u>
1	3.0	25.5	850
2	2.5	19.1	765

The ultimate strengths compare favorably to the 20-psi compressive strength reported for 2-lb density foam (Reference 6, p. 110). This data indicates that a marked decrease in elongation, with little or no increase in ultimate strength, can be expected with this material at cryogenic temperature.

Three specimens of Polyurethane foam were tested, one specimen each at densities of 3-, 6-, and 9-lb/ft³. The test results for these foams are summarized below:

<u>Density, lb/ft³</u>	<u>Deflection, %</u>	<u>Compressive Strength, psi</u>	<u>Modulus, psi</u>
3	1.87	38.1	2030
6	1.25	95.5	7640
9	1.87	151.0	8060

Ultimate compressive strength developed correlate well with data reported for room temperature (Reference 6, p. 131). Again, these data indicate that, at cryogenic temperature, room-temperature ultimate strength is obtained, accompanied by a large reduction in maximum deflection.

Samples of the polyurethane and epoxy foams are shown in Figure 4 after testing.

2. Evaluate for Fabrication and Design Requirements

a. Biaxial Testing Fixture

A biaxial strain fixture was fabricated to verify the analytical design concepts for the liner patterns and establish the strain capability of specific corrugation and pattern geometry. This fixture, with a typical patterned specimen in place, is shown ready for testing in Figure 5. These specimens were tested by marking a 3-in. gage length in each of the principle stress planes and then loading the specimen to strains of 1-1/2 and 2-1/2%. The specimens were fabricated for testing by a rubber forming process. The fabrication sequence is shown in Figure 6.

b. Sample Patterns

Sample patterns of the helix, chevron, crossing, modified crossing, and S-pattern were fabricated. Sketches of these patterns are shown in Figure 7.

It was originally anticipated that these specimens could be strained to 2-1/2% and then cycled to failure. After testing of the first few samples it was apparent that cycling would not be possible because the corners of the specimens would yield during testing and prevent the return of the specimens to its initial gage length. This corner yielding also prevents accurate determination of the stress-strain relationship for each pattern. However, these specimens were evaluated relative to each other. The specimens were rated by neglecting the corner effects and assuming the pattern reduced the biaxial stress to a uniaxial condition. An effective modulus was established for each pattern by

$$E_{\text{eff}} = \frac{\sigma_1}{\epsilon_1}$$

where

σ_1 = principal stress, psi

ϵ_1 = strain in principal stress direction, in./in.

Each of the patterns tested is discussed below and an effective modulus established at 2-1/2 strain or just prior to any buckling. As these specimens were being evaluated one to another, all specimens were fabricated from 3- or 5-mil-thick Type 304 stainless steel.

(1) Helix

The specimen tested was a 45° helix pattern shown after test in Figure 8A. The corrugations had a radius of 1/8-in., with a center spacing of 0.7 in. The specimen reached 2-1/2% strain in the two principle stress planes at a stress level of 6286 psi. This gives an effective modulus of 250,000 psi. Buckling did not occur at any time during the testing. The surface defects shown in the figure were present before testing. A rotation of the pattern of 5° occurred.

(2) Chevron

The chevron pattern tested, shown in Figure 8B, had a corrugation radius of 1/8-in., with a center spacing of 0.7 in. This specimen started buckling at a strain of 1-1/2%. The principle stress at this strain was 8250 psi, giving an effective modulus of 550,000 psi.

(3) Crossing

This specimen was fabricated with a 1/16-in.-radius corrugation on 1-in. centers. The pattern is a basket-weave type with alternating crossovers. At a strain of 2-1/2% a principle stress of 9822 psi was developed, giving an effective modulus of 392,000 psi. Buckling occurred at the top of the crossovers at 2.5% strain. This is illustrated in Figure 8C.

(4) Modified Crossing

The modified crossing pattern is shown in Figure 8D. Buckling of the pattern occurred at a strain just above 2%. Based on a principle stress of 11,700 psi the effective modulus was 585,000 psi. The pattern had corrugations of 1/16-in. radius spaced with 1-in. centers.

(5) S-Pattern

This pattern is shown in Figure 8E. Corrugations have a 1/16-in. radius with a minimum spacing point of 0.25-in. Buckling occurred in this specimen near one corner at a strain of 2%. A principle stress of 7857 psi was developed giving an effective modulus of 390,000 psi.

The effective modulus and strain reached just prior to buckling are summarized for each pattern below:

Pattern	Modulus psi	Strain Prior to Buckling in./in.	Comments
Helix	250,000	0.025	Pattern rotation, 5°
Chevron	550,000	0.015	Buckling at low strain levels
Crossing	392,000	0.025	Buckling at top of crossover
Modified Crossing	585,000	0.020	Highest effective modulus
S-pattern	390,000	0.020	Lowest effective modulus

B. GEOMETRIC ANALYSIS

Selection of specific corrugation dimensions for any given set of design criteria can be much simplified by use of an analysis which will determine the effect of each parameter. The analysis given in the appendix was developed for this purpose. With the computer program developed from the appendix it is possible to evaluate more than 250 different combinations of corrugation parameters per minute.

Approximately 3000 variations in parameters have been investigated, including geometry, materials and support condition. Plots are being made of the various geometry parameters as a function of stress level in order to determine the effects of each variable. Consideration of these parameters in conjunction with dimensions of the initially selected patterns from the biaxial test fixture will define the specific geometry for the 8-in.-dia test vessels.

C. SERIES NUMBER ONE SPECIMEN TEST

The first series of specimen tests consist of the design, fabrication, and testing of eight 8-in.-dia pressure vessels. All of these vessels will be tested in liquid nitrogen.

1. Composite

All specimens will be fabricated with a Dacron-resin composite as discussed in Section III,A,1,a. The basic configuration will be a 8-in.-dia chamber by 12.50 in. long. A 35% boss-to-diameter ratio will be used to facilitate welding of the liner.

2. Liner

Two basic liner patterns will be tested in the first series of specimens. These will be the S-pattern and the crossing pattern. These patterns have been selected on the basis of the biaxial strain tests discussed in Section III,A,2. The S and crossing patterns had the lowest effective modulus of the tested patterns with the exception of the helix. The helix pattern was eliminated because usage in tankage with high length to diameter ratios would

require large rotations of the liner within the composite structure. Final spacing of both patterns will be established from the analytical analysis, as data obtained from the biaxial strain tests are not valid for specific design purpose.

Four different liner types will be fabricated for the first test series. Both liner patterns will be fabricated with each liner type. The liner types are:

- a. Type 304 stainless steel 5-mil-in. thick foil
- b. Type 1100 aluminum, 12-mil-thick foil
- c. Mylar-aluminum laminate, 2-mil Mylar by 1-mil aluminum
- d. Kel-F aluminum laminate, 2-mil Kel-F by 1-mil aluminum.

The polymer aluminum laminates have been selected over polymer films on the basis that laminates in flat sheets have outperformed the straight polymers in previous tests, under NASA Contract NAS 3-2562. The polymer-foil material combinations will minimize permeability problems.

3. Corrugation Support

The analytical analysis has indicated that an elastic support material for the corrugation should have a modulus of approximately 5000 to 10,000 psi and be capable of 5% deflections at cryogenic temperatures. Of the foams tested to date (see Section III,A,1), 6- and 9-lb/ft³ polyurethanes have modulus near the required value; however, deflection at cryogenic temperature was in the range of 1 to 2%. The 2-lb/ft³ density epoxy foams had deflections near 3%, but had extremely low modulus. Before final selection of the back-up material is made, tests will be conducted with a silicone foam material for comparison.

IV. ANTICIPATED WORK FOR NEXT PERIOD

It is anticipated that the following work will be accomplished during the next period:

- A. silicone foam will be evaluated and tested at cryogenic temperatures as a possible corrugation support material.
- B. Designs will be completed for the first series of test specimens.
- C. Fabrication of Series One test specimens will be initiated.

REFERENCES

1. D. C. Hollinger, Influence of Stress Corrosion on Strength of Glass Fibers, First Bi-Monthly Report under Contract NOnr 4486(00)(X), U.S. Naval Research Laboratory.
2. R. P. Reed, "Some Mechanical Properties of Mylar and Dacron Polyester Strands at Low Temperatures," The Review of Scientific Instruments, Vol. 29, No. 8, 734-736, August 1958.
3. Cryogenic Materials Data Handbook, P. B. 171809. U.S. Department of Commerce, Cryogenic Engineering Laboratories, Boulder, Colorado.
4. Coleman J. Major, Karl Hammermeyer, "Gas Permeability of Plastics," Modern Plastics, July 1962.
5. Modern Plastics Encyclopedia, Vol. 41, No. 1A, New York, 1964.
6. "Plastics Reference Issue," Machine Design, September 17, 1964

TABLE 1
RESULTS OF UNIAXIAL TENSION TESTS
(From ASTM E-8*)

<u>Material</u>	<u>Thickness in.</u>	<u>Yield** Strength psi</u>	<u>Ultimate Elongation %</u>
1100 Aluminum	0.006	5,424	31.1
1100 Aluminum	0.008	5,310	35.9
1100 Aluminum	0.012	5,783	37.2
1100 Aluminum	0.016	5,834	36.5
304 Stainless steel	0.003	50,296	29.7
304 Stainless steel	0.005	41,360	46.0
347 Stainless steel	0.003	47,507	21.7
347 Stainless steel	0.006	44,607	31.9

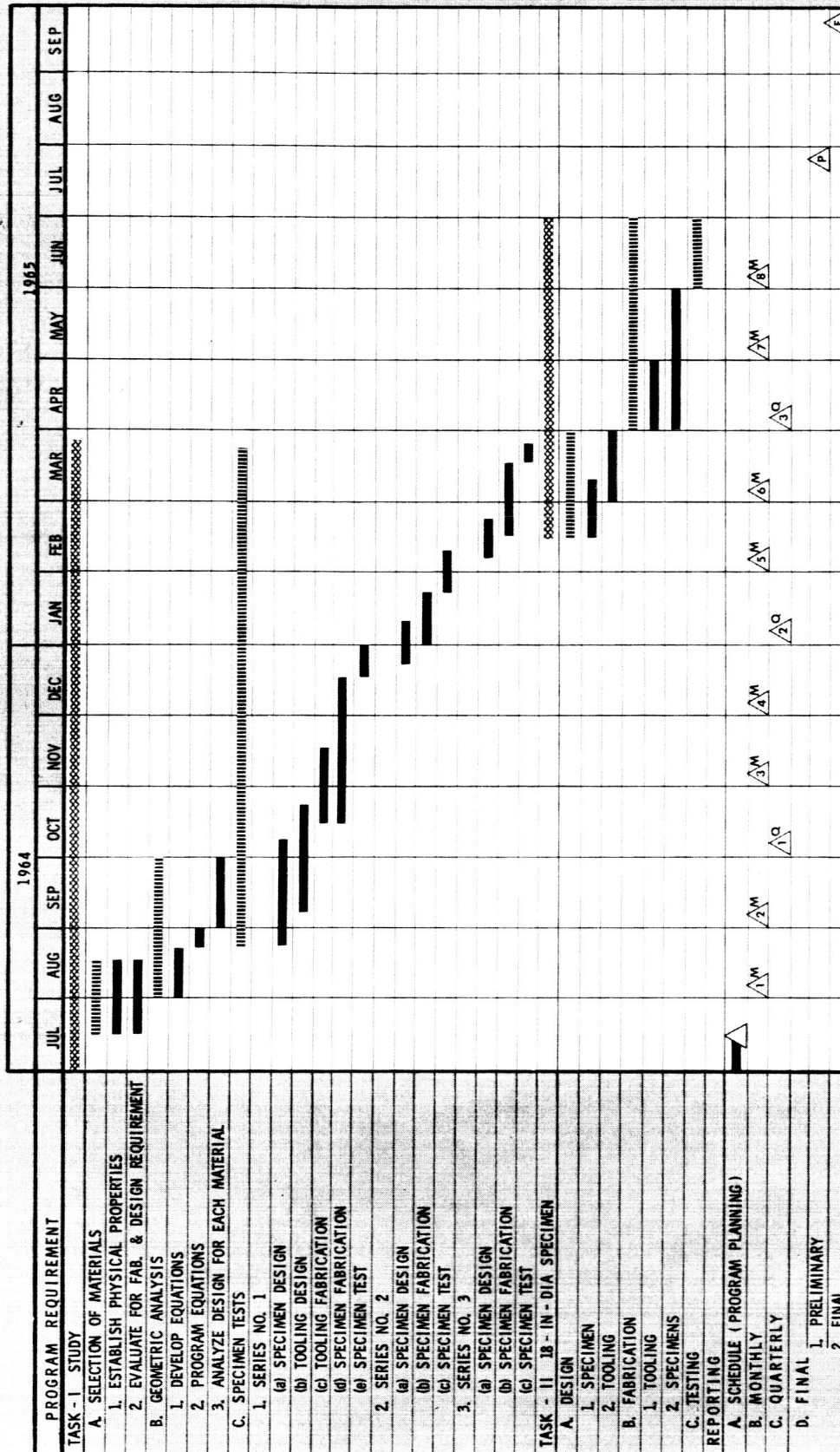
* Each data point is an average of five tensile specimens.

** Yield at 0.2% offset.

Table 1

NASA CONTRACT NAS 3-4189 SUMMARY OF PLANNED PROGRAM

NASA CONTRACT NAS 3-4189



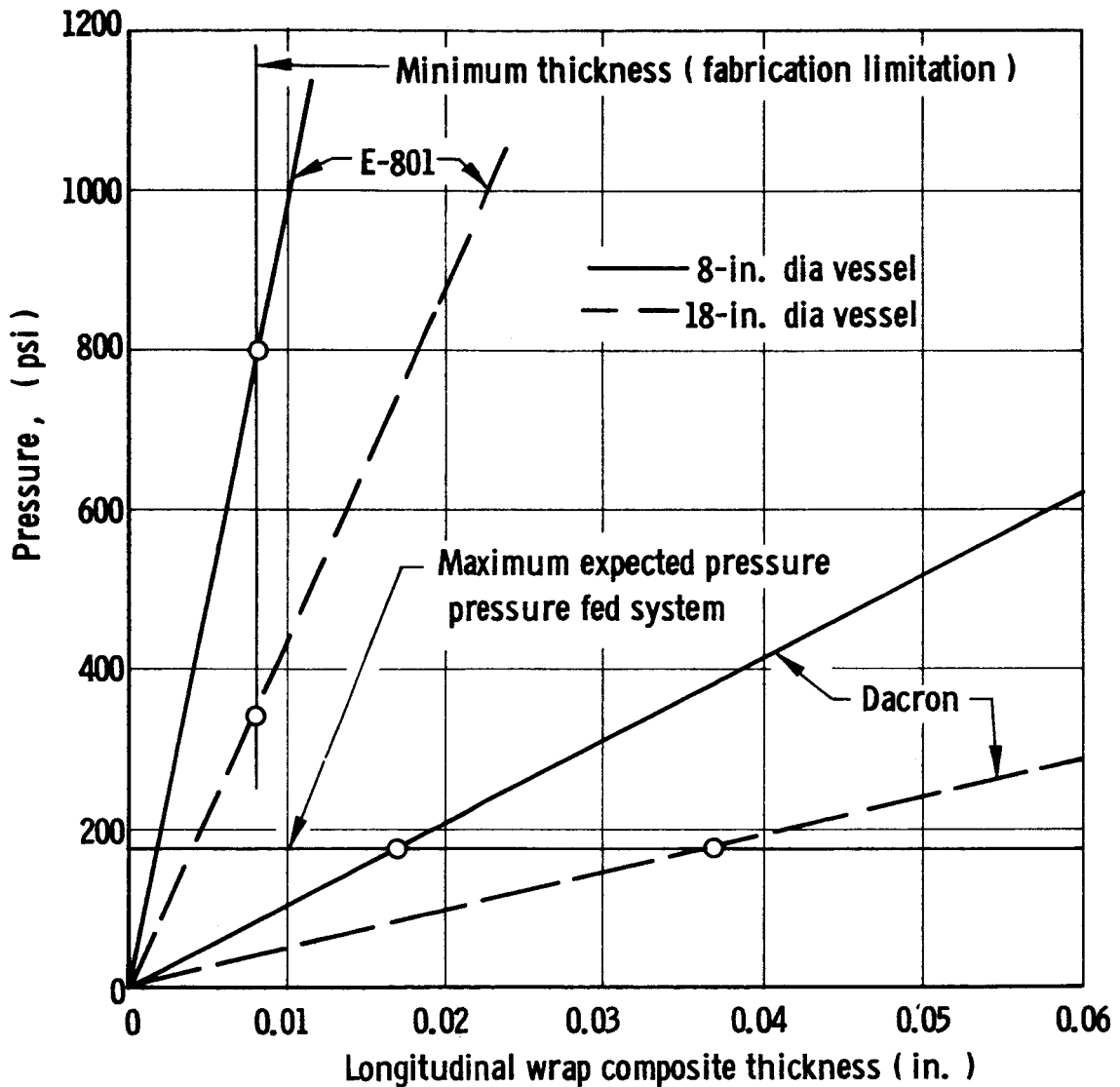
STRUCTURAL MATERIALS DIVISION - VON KARMAN CENTER



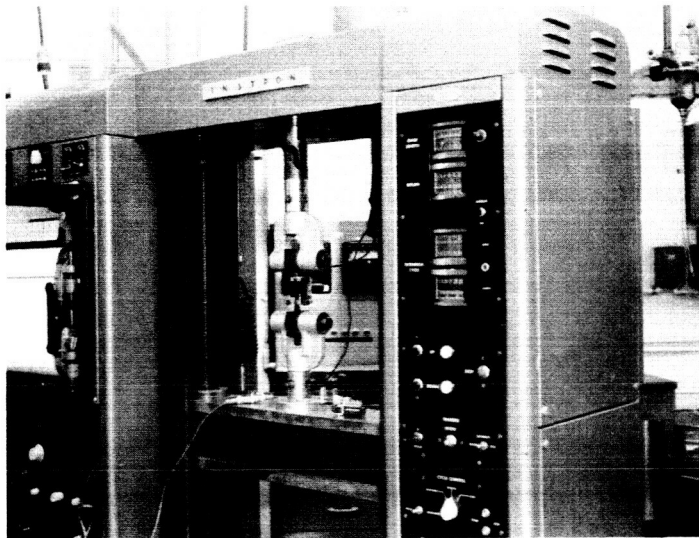
Figure 1



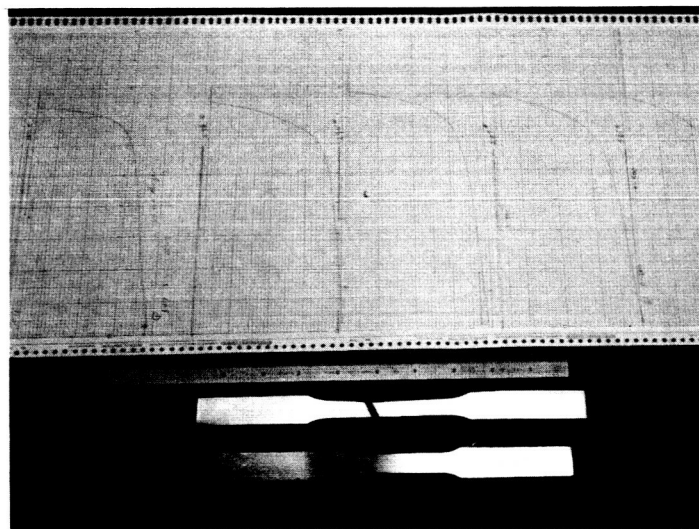
- Note : 1. Glass modulus, $E = 11.88 \times 10^6$ psi (assumed,
 $1.10 \times 10.8 \times 10^6$)
 2. Dacron modulus, $E = 1.3 \times 10^6$ psi



PRESSURE REQUIRED TO ATTAIN 0.025 IN./IN. STRAIN AT
 CRYOGENIC TEMPERATURE VS LONGITUDINAL WRAP THICKNESS

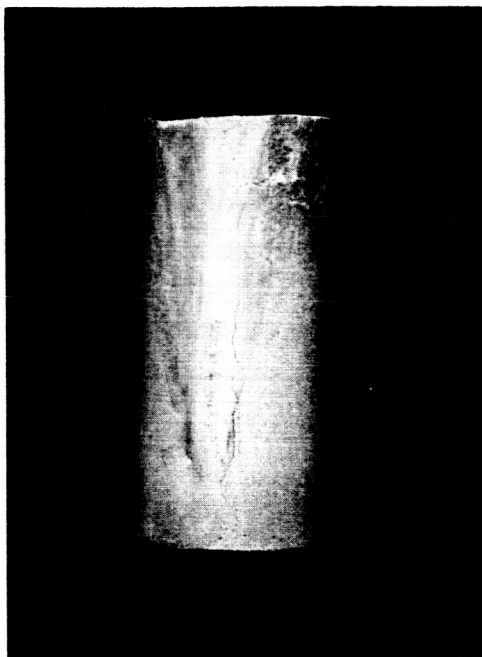


A. Specimen ready for test

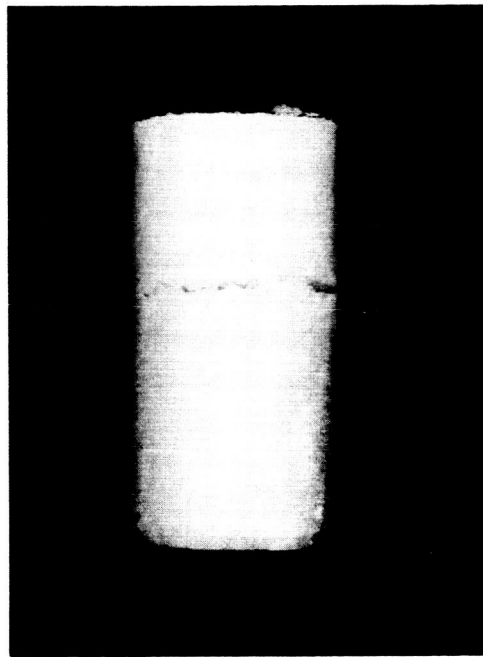


B. 304 stainless steel specimen before and after test with load deflection curve

UNIAXIAL TENSILE SPECIMEN TESTING

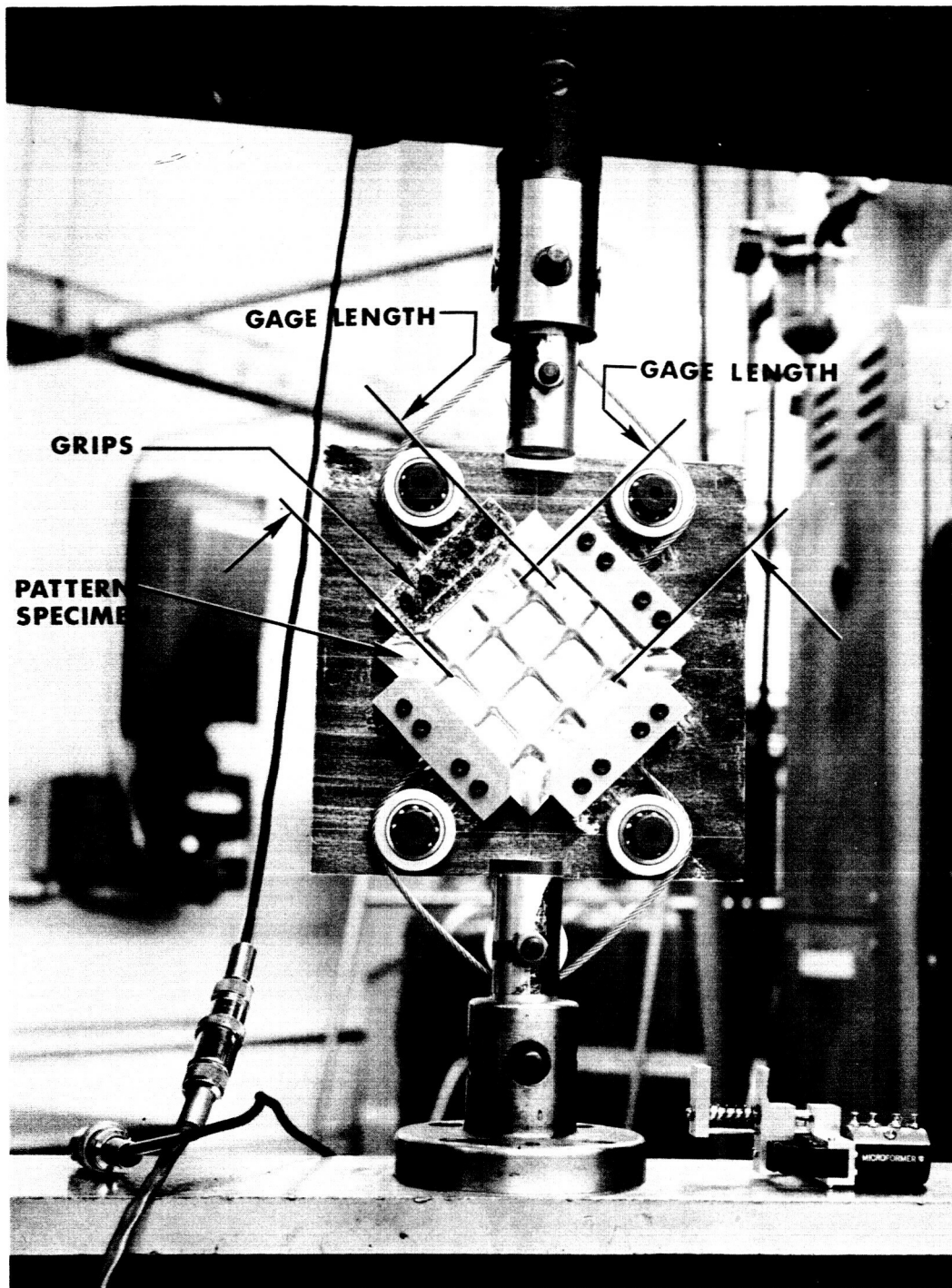


A. Polyurethane Foam



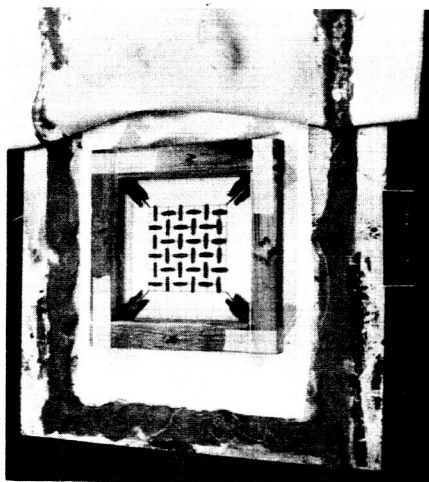
B. Epoxy Foam

POLYURETHANE AND EPOXY FOAM SPECIMENS
AFTER COMPRESSION TEST IN LIQUID NITROGEN

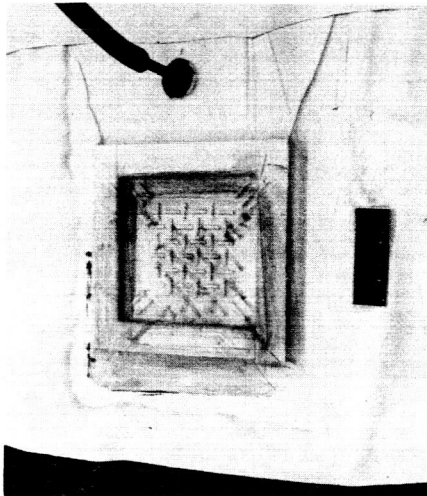


BI AXIAL STRAIN FIXTURE IN INSTRON TENSILE TESTING MACHINE

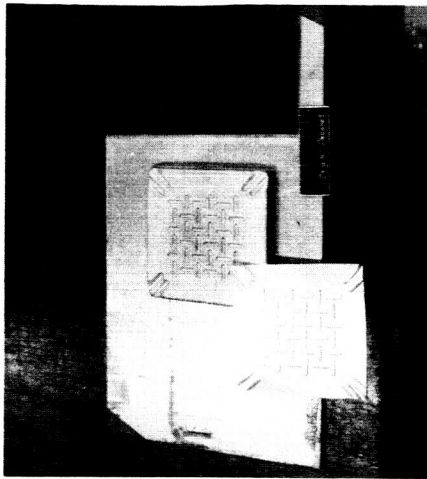
10-067-115



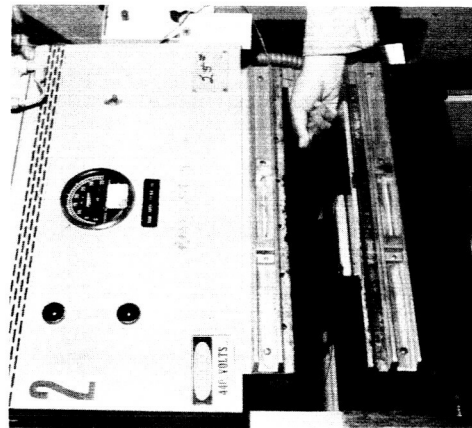
A. Block form with wire pattern



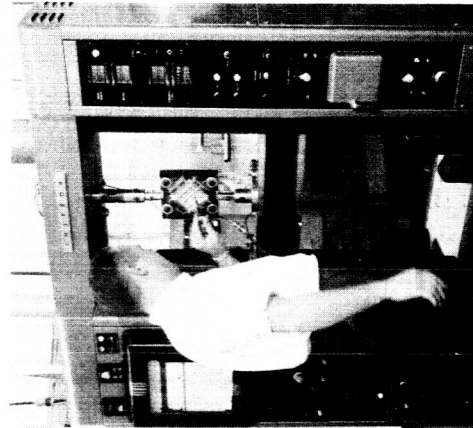
B. Block form covered with vacuum bag



C. Cerrobend mold cast from block form with rubber forming material

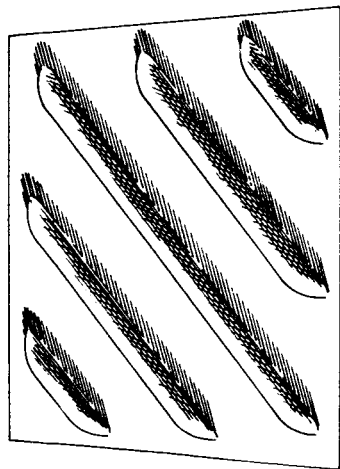


D. Mold and specimen blank in press ready for forming

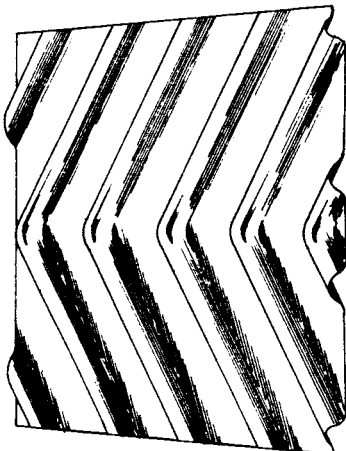


E. Testing specimen in bi-axial strain fixture Instron testing machine

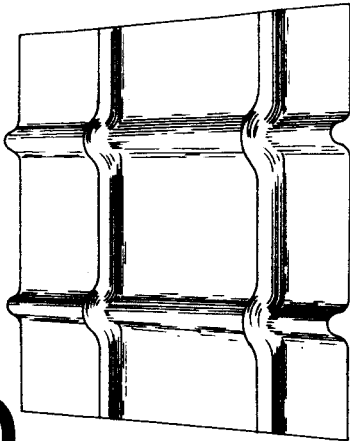
FABRICATION AND TEST PROCEDURE FOR BI-AXIAL STRAIN SPECIMENS



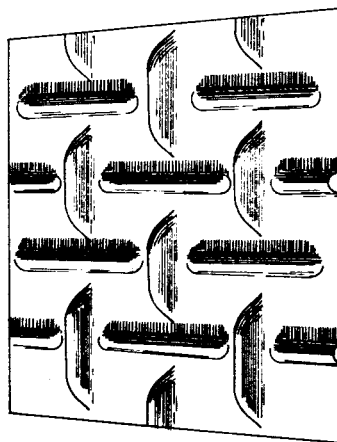
Helix



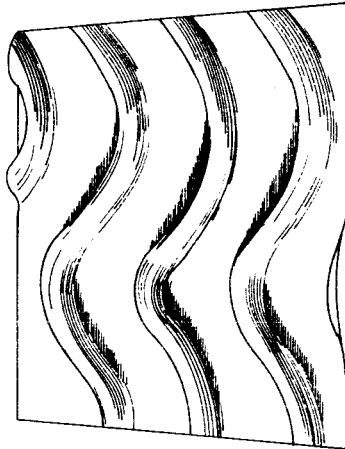
Chevron



Crossing

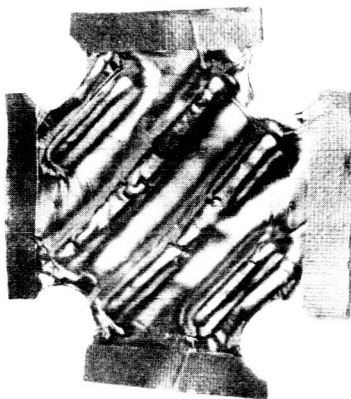


Modified Crossing



"S" Pattern

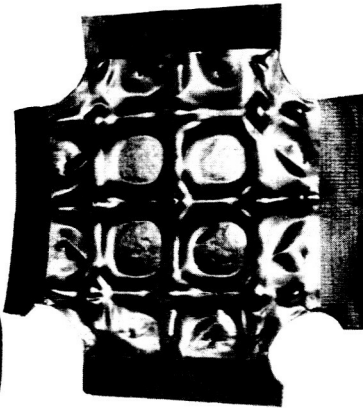
LINER PATTERNS TO BE INVESTIGATED



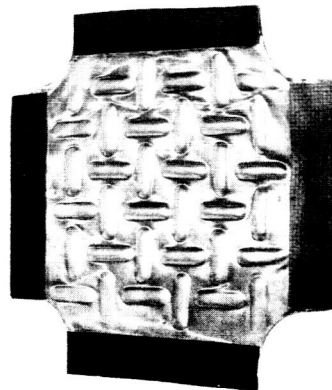
A. Helix



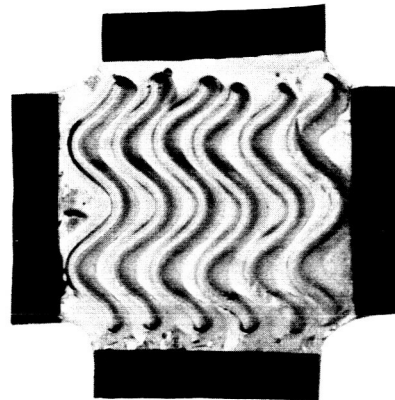
B. Chevron



C. Crossing



D. Modified crossing



E. S-Pattern

SAMPLE LINER PATTERNS AFTER TESTING IN BI-AXIAL STRAIN FIXTURE

APPENDIX

GEOMETRIC ANALYSIS

by

G. A. Lunde

I. OBJECTIVE

This analysis, which predicts stresses and deflections in corrugated liners subjected to combined loadings, was developed in an effort to evaluate possible combinations of liner geometries, materials, and elastic support.

II. SUMMARY

The equations developed in this analysis predict stresses at critical locations of the corrugation, which result from specified lateral deflection and internal pressure. Figure A-1 shows the analytical model and loads considered. This model consists of three sections, convex and concave circular areas and a straight portion. Determination of the effects of support to the back side of the corrugation is accomplished by providing negative uniform pressure loading to the upper circular section.

The analysis has been programmed for digital computation on the IBM 7094. Several thousand possible configurations have been analyzed for both the supported and non-supported conditions. Table A-1 lists the variables considered and the range of each. Evaluation of geometries in this fashion has proven economical because the computer analyzes more than 250 configurations per minute.

Data from the analysis are being evaluated to determine interaction of strain and geometry in order to establish the closest approximation to optimum design.

Rough plots have been made of stress vs the parameters $R\beta$ and t , from the position of the data of the unsupported cases. These plots indicate that all parameters affect the stress picture and that, by careful consideration of each parameter, the specific combination that produces the lowest stress level can be determined. Review of the data from the unsupported configurations indicates that this minimum point lies within the range of parameters evaluated. It should be noted that depending on the orientation of the corrugation with respect to the chamber axis, length of non-corrugated areas, and relative coefficient of expansion, the strain requirement can be magnified greatly, therefore, increasing the stress level. Equations are given, at the end of the analysis, which determine the strain requirement within the corrugation for the magnifying factors.

III. ANALYSIS

Castigliano's theorem for deflection and rotation was utilized in analyzing the model shown in Figure A-1. By use of this theorem, unknown loads at the boundaries of the corrugation are determined. Three distinct regions exist within the corrugation; it is therefore necessary to consider the liner in parts and to then add the parts together to obtain the final load distribution.

A. SECTION ONE - CONCAVE CIRCULAR ARC

1. Horizontal Deflection by Castigliano's Theorem

$$\delta_{HA} = \int \frac{M}{EI} \frac{\partial M}{\partial P_{HA}} R d\phi$$

Since the loads are independent of one another, the deflection can be determined for each separately and subsequently added to the others to determine the total deflection.

a. Horizontal Load (see Figure A-1)

$$M_{PH} = P_{HA} R [\cos \beta - \cos (\beta - \phi)]$$

$$\frac{\partial M}{\partial P_{HA}} = R [\cos \beta - \cos (\beta - \phi)]$$

The theorem assumes a positive deflection in the direction of P_{HA} . However, in this analysis, a positive deflection is in the opposite direction and the sign of $\partial M / \partial P_{HA}$ must be changed.

$$\begin{aligned}\delta_{HA, P_{HA}} &= \frac{1}{EI} \int M_{P_{HA}} \left(- \frac{\partial M}{\partial P_{HA}} \right) R d\phi \\ &= - \frac{1}{EI} \int_0^\beta P_{HA} R^2 [\cos \beta - \cos (\beta - \phi)]^2 d\phi \\ &= - \frac{P_{HA} R^3}{2EI} \left[(1 + 2 \cos^2 \beta) \beta - \frac{3}{2} \sin 2\beta \right]\end{aligned}$$

b. Vertical Load

$$\delta_{HA, P_{VA}} = \frac{1}{EI} \int M_{P_{VA}} \left(- \frac{\partial M}{\partial P_{HA}} \right) R d\phi$$

where

$$\begin{aligned}M_{P_{VA}} &= P_{VA} R [\sin \beta - \sin (\beta - \phi)] \\ \delta_{HA, P_{VA}} &= - \frac{1}{EI} \int_0^\beta P_{VA} R^3 [\sin \beta - \sin (\beta - \phi)] [\cos \beta - \cos (\beta - \phi)] d\phi \\ &= \frac{P_{VA} R^3}{EI} [4 \cos \beta - 2 \beta \sin 2\beta - 3 \cos 2\beta - 1]\end{aligned}$$

c. Bending Moment

$$\begin{aligned}\delta_{HA, M_A} &= \frac{1}{EI} \int M_A \left(- \frac{\partial M}{\partial P_{HA}} \right) R d\phi \\ &= \frac{1}{EI} \int_0^\beta M_A R^2 [\cos \beta - \cos (\beta - \phi)] d\phi \\ &= - \frac{M_A R^2}{EI} [\beta \cos \beta - \sin \beta]\end{aligned}$$

d. Pressure

$$\delta_{HA,p} = \frac{1}{EI} \int M_p - \frac{\partial M}{\partial P_H} R d\phi$$

and

$$\begin{aligned} M_p &= pR^2 [1 - \cos \phi] \\ \delta_{HA,p} &= - \frac{1}{EI} \int_0^\beta pR^4 [1 - \cos \phi] [\cos \beta - \cos (\beta - \phi)] d\phi \\ &= - \frac{pR^4}{EI} [3\beta \cos \beta - \sin 2\beta - \sin \beta] \end{aligned}$$

e. Total Deflection at "A"

$$\delta_{HA} = \delta_{HA,P_{HA}} + \delta_{HA,P_{VA}} + \delta_{HA,M_A} + \delta_{HA,p} \quad (1)$$

2. Vertical Deflection

$$\delta_{VA} = \int_0^\beta \frac{M}{EI} \frac{\partial M}{\partial P_{VA}} R d\phi$$

$$M_{P_{VA}} = P_{VA} R [\sin \beta - \sin (\beta - \phi)]$$

$$\frac{\partial M}{\partial P_{VA}} = R [\sin \beta - \sin (\beta - \phi)]$$

a. Horizontal Load

$$\begin{aligned} \delta_{VA,P_{HA}} &= \frac{1}{EI} \int M_{P_{HA}} \frac{\partial M}{\partial P_{VA}} R d\phi \\ &= \frac{1}{EI} \int_0^\beta P_{HA} R^3 [\cos \beta - \cos (\beta - \phi)] \\ &\quad [\sin \beta - \sin (\beta - \phi)] d\phi \\ &= \frac{P_{HA} R^3}{EI} [2\beta \sin 2\beta - 4 \cos \beta + 3 \cos 2\beta + 1] \end{aligned}$$

b. Vertical Load

$$\begin{aligned}
 \delta_{VA, P_{VA}} &= \frac{1}{EI} \int M_{P_{VA}} \frac{\partial M}{\partial P_{VA}} R d\phi \\
 &= \frac{1}{EI} \int_0^{\beta} P_{VA} R^3 [\sin \beta - \sin (B - \phi)]^2 d\phi \\
 &= \frac{P_{VA} R^3}{EI} \left[\beta (1 + 2 \sin^2 \beta) - 4 \sin \beta + \frac{3}{2} \sin 2\beta \right]
 \end{aligned}$$

c. Bending Moment

$$\begin{aligned}
 \delta_{VA, M_A} &= \frac{1}{EI} \int M_A \frac{\partial M}{\partial P_{VA}} R d\phi \\
 &= \frac{1}{EI} \int_0^{\beta} M_A R^2 [\sin \beta - \sin (B - \phi)] d\phi \\
 &= \frac{M_A R^2}{EI} [\beta \sin \beta - 1 + \cos \beta]
 \end{aligned}$$

d. Pressure

$$\begin{aligned}
 \delta_{VA, p} &= \frac{1}{EI} \int M_P \frac{\partial M}{\partial P_{VA}} R d\phi \\
 &= \frac{1}{EI} \int_0^{\beta} p R^4 (1 - \cos \phi) [\sin \beta - \sin (\beta - \phi)] d\phi \\
 &= \frac{p R^4}{EI} \left[\frac{3\beta}{2} \sin \beta - (1 + \sin^2 \beta) + \cos \beta \right]
 \end{aligned}$$

e. Total Vertical Displacement at "A"

$$\delta_{VA} = \delta_{VA, P_{HA}} + \delta_{VA, P_{VA}} + \delta_{VAM, A} + \delta_{VA, p} \quad (2)$$

3. Rotation

$$\theta_A = \int \frac{M}{EI} \cdot \frac{\partial M}{\partial M_A} R d\phi$$

$$M_A = M_A$$

$$\frac{\partial M}{\partial M_A} = 1$$

a. Horizontal Load

$$\begin{aligned} \theta_{A, P_{HA}} &= \frac{1}{EI} \int M_{P_{HA}} \frac{\partial M}{\partial M_A} R d\phi \\ &= \frac{1}{EI} \int_0^\beta P_{VA} R^2 [\cos \beta - \cos (\beta - \phi)] d\phi \\ &= \frac{P_{HA} R^2}{EI} [\beta \cos \beta - \sin \beta] \end{aligned}$$

b. Vertical Load

$$\begin{aligned} \theta_{A, P_{VA}} &= \frac{1}{EI} \int M_{P_{VA}} \frac{\partial M}{\partial M_A} R d\phi \\ &= \frac{1}{EI} \int_0^\beta P_{VA} R^2 [\sin \beta - \sin (\beta - \phi)] d\phi \\ &= \frac{P_{VA} R^2}{EI} [\cos \beta + \beta \sin \beta - 1] \end{aligned}$$

c. Moment

$$\begin{aligned} \theta_{A, M_A} &= \frac{1}{EI} \int M_A \frac{\partial M}{\partial M_A} R d\phi \\ &= \frac{1}{EI} \int_0^\beta M_A R d\phi = \frac{M_A R}{EI} (\beta) \end{aligned}$$

d. Pressure

$$\begin{aligned}
 \theta_{A,p} &= \frac{1}{EI} \int M_p \frac{\partial M}{\partial M_A} R d\phi \\
 &= \frac{1}{EI} \int_0^\beta p R^3 [1 - \cos \phi] d\phi \\
 &= \frac{p R^3}{EI} [\beta - \sin \beta]
 \end{aligned}$$

e. Total Rotation at "A"

$$\theta_A = \theta_{A,P_{HA}} + \theta_{A,P_{VA}} + \theta_{A,M_A} + \theta_{A,p}$$

B. SECTION II - STRAIGHT PORTION

1. Horizontal Deflection

$$\delta_{HB} = \delta_{HA} + [L \sin \beta] \theta_A + \int \frac{M}{EI} \left(- \frac{\partial M}{\partial P_{HB}} \right) ds$$

$$M_{P_{HB}} = - P_{HB} S \sin \beta$$

$$\frac{\partial M}{\partial P_{HB}} = - S \sin \beta$$

$$M = P_{HB} S \sin \beta + P_{VB} S \cos \beta + M_B + \frac{p S^2}{2}$$

Because of the simplicity of this moment equation, the integration will be carried out for all loads at one time.

$$\begin{aligned}
 I_{HB} &= \int - \frac{M}{EI} \left(\frac{\partial M}{\partial P_{HB}} \right) dS \\
 &= \frac{1}{EI} \int_0^L \left(- P_{HB} S \sin \beta + P_{VB} S \cos \beta + M_B + \frac{p S^2}{2} \right) (S \sin \beta) dS \\
 &= \frac{1}{EI} \left[- \frac{P_{HB} L^3 \sin \beta}{3} + \frac{P_{VB} L^3 \cos \beta \sin \beta}{3} + \frac{M_B L^2 \sin \beta}{2} + \right. \\
 &\quad \left. \frac{p L^4 \sin \beta}{8} \right]
 \end{aligned}$$

$$\delta_{HB} = \delta_{HA} + (L \sin \beta) \theta_A + I_{HB} \quad (4)$$

2. Vertical Deflection

$$\delta_{VB} = \delta_{VA} + (L \cos \beta) \theta_A + \int \frac{M}{EI} \frac{\partial M}{\partial P_{VB}} dS$$

$$\frac{\partial M}{\partial P_{VB}} = S \cos \beta$$

$$I_{VB} = \int \frac{M}{EI} \frac{\partial M}{\partial P_{VB}} dS$$

$$I_{VB} = \frac{1}{EI} \int_0^L \left(-P_{HB} S \sin \beta + P_{VB} S \cos \beta + M_B + \frac{pS^2}{2} \right) (S \cos \beta) dS$$

$$= \frac{1}{EI} \left[-\frac{P_{HB} L^3 \sin \beta \cos \beta}{3} + \frac{P_{VB} L^3 \cos^2 \beta}{3} + \frac{M_B L^2 \cos \beta}{2} + \frac{pL^4 \cos \beta}{8} \right]$$

$$\delta_{VB} = \delta_{VA} + (L \cos \beta) \theta_A + I_{VB} \quad (5)$$

3. Rotation

$$\theta_B = \theta_A + \int \frac{M}{EI} \frac{\partial M}{\partial M_B} dS$$

$$\frac{\partial M}{\partial M_B} = 1$$

$$I_{\theta} = \int \frac{M}{EI} \frac{\partial M}{\partial M_B} dS = \frac{1}{EI} \int_0^L \left(-P_{HB} S \sin \beta + P_{VB} S \cos \beta + M_B + \frac{pS^2}{2} \right) dS$$

$$= \frac{1}{EI} \left[-\frac{P_{HB} L^2 \sin \beta}{2} + \frac{P_{VB} L^2 \cos \beta}{2} + M_B L + \frac{pL^3}{6} \right]$$

$$\theta_B = \theta_A + I_{\theta}$$

C. SECTION III - CONVEX CIRCULAR ARC

1. Horizontal Deflection

$$\delta_{HO} = \delta_{HB} + R (1 - \cos \beta) \theta_B + \int \frac{M}{EI} \left(- \frac{\partial M}{\partial P_{HO}} \right) R d\phi$$

$$M_{P_{HO}} = - P_{HO} R (1 - \cos \phi)$$

$$\frac{\partial M}{\partial P_{HO}} = - R (1 - \cos \phi)$$

a. Horizontal Load

$$\begin{aligned} \delta_{HO, P_{HO}} &= \frac{1}{EI} \int M_{P_{HO}} \left(- \frac{\partial M}{\partial P_{HO}} \right) R d\phi \\ &= - \frac{1}{EI} \int_0^\beta P_{HO} R^3 [1 - \cos \phi]^2 d\phi \\ &= - \frac{P_{HO} R^3}{EI} \left[\frac{3}{2} \beta - 2 \sin \beta + \frac{1}{4} \sin 2 \beta \right] \end{aligned}$$

b. Vertical Load

$$M_{P_{VO}} = P_{VO} R \sin \phi$$

$$\begin{aligned} \delta_{HO, P_{VO}} &= \frac{1}{EI} \int M_{P_{VO}} \left(- \frac{\partial M}{\partial P_{HO}} \right) R d\phi \\ &= \frac{1}{EI} \int_0^\beta P_{VO} R^3 (\sin \phi) (1 - \cos \phi) d\phi \\ &= \frac{P_{VO} R^3}{EI} \left[\frac{3}{4} \cos \beta + \frac{1}{4} \cos 2 \beta \right] \end{aligned}$$

c. Bending Moment

$$\begin{aligned}
 \delta_{HO, M_O} &= \frac{1}{EI} \int M_O \frac{\partial M}{\partial P_{HO}} R d\phi \\
 &= \frac{1}{EI} \int_0^\beta M_O R^2 (1 - \cos \phi) d\phi \\
 &= \frac{M_O R^2}{EI} [\beta - \sin \beta]
 \end{aligned}$$

d. Pressure

In order to include the effects of support on the back side of the corrugation, it will be assumed that the support reacts with a uniform radial pressure over the back side of the convex circular arc. This effect is included simply by multiplying the pressure, p , by a factor, γ , which is dependent upon the supporting condition. For the condition of no support $\gamma = 1$ while for 90° corrugations or those with no straight portion $\gamma = -1$ will provide a support that reacts the total vertical load caused by the pressure. Other values of γ chosen properly will provide for support when a straight portion is used.

$$\begin{aligned}
 M_P &= \gamma p R^2 (1 - \cos \phi) \\
 \delta_{HO, P} &= \frac{1}{EI} \int M_P \frac{\partial M}{\partial P_{HO}} R d\phi \\
 &= \frac{1}{EI} \int_0^\beta \gamma p R^4 (1 - \cos \phi)^2 d\phi \\
 &= \frac{\gamma p R^4}{EI} \left[\frac{3}{2} \beta - 2 \sin \beta + \frac{1}{4} \sin 2 \beta \right]
 \end{aligned}$$

e. Total Horizontal Deflection at "O"

$$\delta_{HO} = \delta_{HB} + R (1 - \cos \beta) \theta_B + \delta_{HO, P_{HO}} + \delta_{HO, P_{VO}} + \delta_{HO, M_O} + \delta_{HO, P} \quad (7)$$

2. Vertical Deflection

$$\delta_{VO} = \delta_{VB} + (R \sin \beta) \theta_B + \int \frac{M}{EI} \frac{\partial M}{\partial P_{VO}} R d\phi$$

$$\frac{\partial M}{\partial P_{VO}} = R \sin \phi$$

a. Horizontal Load

$$\begin{aligned} \delta_{VO, P_{HO}} &= \frac{1}{EI} \int M_{P_{HO}} \frac{\partial M}{\partial P_{VO}} R d\phi \\ &= \frac{1}{EI} \int_0^\beta -P_{HO} R^3 (1 - \cos \phi) \sin \phi d\phi \\ &= -\frac{P_{HO} R^3}{EI} \left[\frac{3}{4} - \cos \beta + \frac{1}{4} \cos 2\beta \right] \end{aligned}$$

b. Vertical Load

$$\begin{aligned} \delta_{VO, P_{VO}} &= \frac{1}{EI} \int M_{P_{VO}} \frac{\partial M}{\partial P_{VO}} R d\phi \\ &= \frac{1}{EI} \int_0^\beta P_{VO} R^3 \sin^2 \phi d\phi \\ &= \frac{P_{VO} R^3}{EI} \left[\frac{\beta}{2} - \frac{1}{4} \sin 2\beta \right] \end{aligned}$$

c. Moment

$$\begin{aligned}
 \delta_{VO, M_O} &= \frac{1}{EI} \int M_O \frac{\partial M}{\partial P_{VO}} R d\phi \\
 &= \frac{1}{EI} \int_0^\beta M_O R^2 \sin \phi d\phi \\
 &= \frac{M_O R^2}{EI} [1 - \cos \beta]
 \end{aligned}$$

d. Pressure

$$\begin{aligned}
 \delta_{VO, P} &= \frac{1}{EI} \int M_P \frac{\partial M}{\partial P_{VO}} R d\phi \\
 &= \frac{1}{EI} \int_0^\beta \gamma P R^4 (1 - \cos \phi) \sin \phi d\phi \\
 &= \frac{\gamma P R^4}{EI} \left[\frac{3}{4} - \cos \beta + \frac{1}{4} \cos 2\beta \right]
 \end{aligned}$$

e. Total Vertical Deflection at "O"

$$\begin{aligned}
 \delta_{VO} &= \delta_{VB} + (R \sin \beta) \theta_B + \delta_{VO, P_{HO}} + \delta_{VO, P_{VO}} + \\
 &\quad \delta_{VO, M_O} + \delta_{VO, P}
 \end{aligned} \tag{8}$$

3. Rotation

$$\theta_O = \theta_B + \int \frac{M}{EI} \frac{\partial M}{\partial M_O} R d\phi$$

$$\frac{\partial M}{\partial M_O} = 1$$

a. Horizontal Load

$$\begin{aligned}
 \theta_{O, P_{HO}} &= \frac{1}{EI} \int M_{P_{HO}} \frac{\partial M}{\partial M_O} R d\phi \\
 &= \frac{1}{EI} \int_0^\beta -P_{HO} R^2 (1 - \cos \phi) d\phi \\
 &= -\frac{P_{HO} R^2}{EI} \left[\beta - \sin \beta \right]
 \end{aligned}$$

b. Vertical Load

$$\begin{aligned}
 \theta_{O, P_{VO}} &= \frac{1}{EI} \int M_{P_{VO}} \frac{\partial M}{\partial M_O} R d\phi \\
 &= \frac{1}{EI} \int_0^\beta P_{VO} R^2 (\sin \phi) d\phi \\
 &= \frac{P_{VO} R^2}{EI} (1 - \cos \beta)
 \end{aligned}$$

c. Bending Moment

$$\begin{aligned}
 \theta_{O, M_O} &= \frac{1}{EI} \int M_O \frac{\partial M}{\partial M_O} R d\phi \\
 &= \frac{1}{EI} \int_0^\beta M_O R d\phi \\
 &= \frac{M_O R}{EI} (\beta)
 \end{aligned}$$

d. Pressure

$$\begin{aligned}\theta_{O,p} &= \frac{1}{EI} \int M_P \frac{\partial M}{\partial M_O} R d\phi \\ &= \frac{1}{EI} \int_0^\beta \gamma P R^3 (1 - \cos \phi) d\phi \\ &= \frac{\gamma P R^3}{EI} [\beta - \sin \beta]\end{aligned}$$

e. Total Rotation at "O"

$$\theta_O = \theta_B + \theta_{O,P_{HO}} + \theta_{O,P_{VO}} + \theta_{O,M_O} + \theta_{O,p} \quad (9)$$

D. DETERMINATION OF INTERNAL LOADS

The forces P_{HO} , P_{VO} , and M_O result from the corrugation being deformed by the applied pressure. The other unknown forces, P_{HB} , P_{VB} , M_B , P_{HA} , P_{VA} , and M_A also result from the deformation, but can be expressed as a function of the loads at "O" and the pressure by equations from statics. It remains therefore to determine the loads at "O" which is done by evaluating Equations (7), (8), and (9) after they are expressed in terms of P_{HO} , P_{VO} , and M_O . Evaluation of the above equations is possible because the following quantities at "O" are known

$$\delta_{H,O} = \text{constant}$$

$$\theta_O = 0$$

$$P_{VO} = 0$$

If a local rigid support is desired at "O" then $\delta_{VO} = \text{constant}$ and P_{VO} becomes an unknown.

1. Substitution of Variables into Section I by Statics
(see Figure A-1)

$$P_{HA} = P_{HO} - p [L \sin \beta + \gamma R (1 - \cos \beta)]$$

let

$$C_1 = 1$$

$$K_1 = - [L \sin \beta + \gamma R (1 - \cos \beta)]$$

then

$$P_{HA} = C_1 P_{HO} + K_1 p \tag{10}$$

$$\begin{aligned} P_{VA} &= P_{VO} + p [L \cos \beta + \gamma R (\sin \beta)] \\ &= C_1 P_{VO} + K_2 p \end{aligned} \tag{11}$$

where

$$\begin{aligned}
 K_2 &= L \cos \beta + \gamma R \sin \beta \\
 M_A &= M_0 - P_{HO} [R (1 - \cos \beta) + L \sin \beta] + P_{VO} (R \sin \beta + L \cos \beta) \\
 &\quad + p \left[R^2 (1 - \cos \beta) + RL \sin \beta + \frac{L^2}{2} \right] \\
 &= C_1 M_0 + C_2 P_{HO} + C_3 P_{VO} + K_3
 \end{aligned} \tag{12}$$

where

$$\begin{aligned}
 C_2 &= - [R (1 - \cos \beta) + L \sin \beta] \\
 C_3 &= R \sin \beta + L \cos \beta \\
 K_3 &= \gamma \left[R^2 (1 - \cos \beta) + RL \sin \beta \right] + \frac{L^2}{2}
 \end{aligned}$$

a. Horizontal Deflection

From Equation (1)

$$\delta_{HA} = C_4 P_{HA} + C_5 P_{VA} + C_6 M_A + K_4 p$$

where

$$\begin{aligned}
 C_4 &= - \frac{R^3}{2EI} \left[(1 + 2 \cos^2 \beta) \beta - \frac{3}{2} \sin \beta \right] \\
 C_5 &= \frac{R^3}{EI} (4 \cos \beta - 2\beta \sin 2\beta - 3 \cos 2\beta - 1) \\
 C_6 &= \frac{R^2}{EI} (\sin \beta - \beta \cos \beta) \\
 K_4 &= \frac{R^4}{EI} (3\beta \cos \beta - \sin 2\beta - \beta) \\
 \delta_{HA} &= C_4 (C_1 P_{HO} + K_1 p) + C_5 (C_1 P_{VO} + K_2 p) \\
 &\quad + C_6 (C_1 M_0 + C_2 P_{HO} + C_3 P_{VO} + K_3 p) + K_4 p \\
 &= S_1 P_{HO} + S_2 P_{VO} + S_3 M_0 + D_1 p
 \end{aligned} \tag{13}$$

where

$$S_1 = C_1 C_4 + C_2 C_6$$

$$S_2 = C_1 C_5 + C_3 C_6$$

$$S_3 = C_1 C_6$$

$$D_1 = K_1 C_4 + K_2 C_5 + K_3 C_6 + K_4$$

b. Vertical Deflection

From Equation (2)

$$\delta_{VA} = C_7 P_{HA} + C_8 P_{VA} + C_9 M_A + K_5 P$$

where

$$C_7 = \frac{R^3}{EI} (2\beta \sin 2\beta - 4 \cos \beta + 3 \cos 2\beta + 1)$$

$$C_8 = \frac{R^3}{EI} \left[\beta (1 + 2 \sin^2 \beta) - 4 \sin \beta + \frac{3}{2} \sin 2\beta \right]$$

$$C_9 = \frac{R^2}{EI} (\beta \sin \beta - 1 + \cos \beta)$$

$$K_5 = \frac{R^4}{EI} \left[\frac{3\beta}{2} \sin \beta - (1 + \sin^2 \beta) + \cos \beta \right]$$

$$\begin{aligned} \delta_{VA} &= C_7 (C_1 P_{HO} + K_1 P) + C_8 (C_1 P_{VO} + K_2 P) \\ &\quad + C_9 (C_1 M_O + C_2 P_{HO} + C_3 P_{VO} + K_3 P) + K_5 P \\ &= S_4 P_{HO} + S_5 P_{VO} + S_6 M_O + D_2 P \end{aligned} \quad (14)$$

where

$$S_4 = C_1 C_7 + C_2 C_9$$

$$S_5 = C_1 C_8 + C_3 C_9$$

$$S_6 = C_1 C_9$$

$$D_2 = K_1 C_7 + K_2 C_8 + K_3 C_9 + K_5$$

c. Rotation

From Equation (3)

$$\theta_A = C_{10} P_{HA} + C_{11} P_{VA} + C_{12} M_A + K_6 p$$

$$C_{10} = \frac{R^2}{EI} (\beta \cos \beta - \sin \beta)$$

$$C_{11} = \frac{R^2}{EI} (\cos \beta + \beta \sin \beta - 1)$$

$$C_{12} = \frac{R\beta}{EI}$$

$$K_6 = \frac{R^3}{EI} (\beta - \sin \beta)$$

$$\begin{aligned} \theta_A &= C_{10} (C_1 P_{HO} + K_1 p) + C_{11} (C_1 P_{VO} + K_2 p) \\ &\quad + C_{12} (C_1 M_O + C_2 P_{HO} + C_3 P_{VO} + K_3 p) + K_6 p \\ &= S_7 P_{HO} + S_8 P_{VO} + S_9 M_O + D_3 p \end{aligned} \quad (15)$$

where

$$S_7 = C_1 C_{10} + C_2 C_{12}$$

$$S_8 = C_1 C_{11} + C_3 C_{12}$$

$$S_9 = C_1 C_{12}$$

$$D_3 = K_1 C_{10} + K_2 C_{11} + K_3 C_{12} + K_6$$

2. Substitution of Variables into Section II by Statics
(see Figure A-2)

$$\begin{aligned} P_{HB} &= P_{HO} - \gamma p R (1 - \cos \beta) \\ &= C_{11} P_{HO} + K_7 p \end{aligned} \quad (16)$$

$$K_7 = -\gamma (1 - \cos \beta) R$$

$$\begin{aligned} P_{VB} &= P_{VO} + \gamma p R \sin \beta \\ &= C_{11} P_{VO} + K_8 p \end{aligned} \quad (17)$$

where

$$K_8 = \gamma R \sin \beta$$

$$\begin{aligned} M_B &= M_O - P_{HO} R (1 - \cos \beta) + P_{VO} R \sin \beta + \gamma p R^2 (1 - \cos \beta) \\ &= C_{11} M_O + C_{13} P_{HO} + C_{14} P_{VO} + K_9 p \end{aligned} \quad (18)$$

where

$$C_{13} = -R (1 - \cos \beta)$$

$$C_{14} = R \sin \beta$$

$$K_9 = \gamma R^2 (1 - \cos \beta)$$

a. Horizontal Deflection

From Equation (4)

$$\delta_{HB} = \delta_{HA} + C_{15} \theta_A + C_{16} P_{HB} + C_{17} P_{VB} + C_{18} M_B + K_{10} p$$

where

$$C_{15} = L \sin \beta$$

$$C_{16} = -\frac{L^3 \sin \beta}{3EI}$$

$$C_{17} = \frac{C^3 \cos \beta \sin \beta}{3EI}$$

$$C_{18} = \frac{L^2 \sin \beta}{2EI}$$

$$K_{10} = \frac{L^4 \sin \beta}{8EI}$$

$$\begin{aligned} \delta_{HB} &= S_1 P_{HO} + S_2 P_{VO} + S_3 M_O + D_1 p + C_{15} (S_7 P_{HO} + S_8 P_{VO} \\ &\quad + S_9 M_O + D_3 p) + C_{16} (C_1 P_{HO} + K_7 p) + C_{17} (C_1 P_{VO} \\ &\quad + K_8 p) + C_{18} (C_1 M_O + C_{13} P_{HO} + C_{14} P_{VO} + K_9 p) + K_{10} p \\ &= S_{10} P_{HO} + S_{11} P_{VO} + S_{12} M_O + D_4 p \end{aligned} \quad (19)$$

where

$$S_{10} = C_1 C_{16} + C_{13} C_{18} + S_1 + C_{15} S_7$$

$$S_{11} = C_1 C_{17} + C_{14} C_{18} + S_2 + C_{15} S_8$$

$$S_{12} = C_1 C_{18} + S_3 + C_{15} S_9$$

$$D_4 = K_7 C_{16} + K_8 C_{17} + K_9 C_{18} + D_1 + C_{15} D_3 + K_{10}$$

b. Vertical Deflection

From Equation (5)

$$\delta_{VB} = \delta_{VA} + C_{19} \theta_A + C_{20} P_{HB} + C_{21} P_{VB} + C_{22} M_B + K_{11} p$$

where

$$C_{19} = L \cos \beta$$

$$C_{20} = - \frac{L^3 \sin \beta \cos \beta}{3EI}$$

$$C_{21} = \frac{L^3 \cos^2 \beta}{3EI}$$

$$C_{22} = \frac{L^2 \cos \beta}{2EI}$$

$$K_{11} = \frac{L^4 \cos \beta}{8EI}$$

$$\begin{aligned} \delta_{VB} &= S_4 P_{HO} + S_5 P_{VO} + S_6 M_O + D_2 p + C_{19} (S_7 P_{HO} + S_8 P_{VO} \\ &\quad + S_9 M_O + D_3 p) + C_{20} (C_1 P_{HO} + K_7 p) + C_{21} (C_1 P_{VO} + K_8 p) \\ &\quad + C_{22} (C_1 M_O + C_{13} P_{HO} + C_{14} P_{VO} + K_9 p) + K_{11} p \\ &= S_{13} P_{HO} + S_{14} P_{VO} + S_{15} M_O + D_5 \end{aligned} \quad (20)$$

where

$$S_{13} = C_1 C_{20} + C_{13} C_{22} + S_4 + C_{19} S_7$$

$$S_{14} = C_1 C_{21} + C_{14} C_{22} + S_5 + C_{19} S_8$$

$$S_{15} = C_1 C_{22} + S_6 + C_{19} S_9$$

$$D_5 = K_7 C_{20} + K_8 C_{21} + K_9 C_{22} + D_2 + C_{19} D_3 + K_{10}$$

c. Rotation

From Equation (6)

$$\theta_B = \theta_A + C_{23} P_{HB} + C_{24} P_{VB} + C_{25} M_B + K_{12} p$$

where

$$C_{23} = - \frac{L^2 \sin \beta}{2EI}$$

$$C_{24} = \frac{L^2 \cos \beta}{2EI}$$

$$C_{25} = \frac{L}{EI}$$

$$K_{12} = \frac{L^3}{6EI}$$

$$\begin{aligned} \theta_B &= S_7 P_{HO} + S_8 P_{VO} + S_9 M_0 + D_3 + C_{23} (C_1 P_{HO} + K_7 P) \\ &\quad + C_{24} (C_1 P_{VO} + K_2 P) + C_{25} (C_1 M_0 + C_{13} P_{HO} + C_{14} P_{VO} \\ &\quad + K_9 P) + K_{12} P \\ &= S_{16} P_{HO} + S_{17} P_{VO} + S_{18} M_0 + D_6 \end{aligned} \quad (21)$$

where

$$S_{16} = C_1 C_{23} + C_{13} C_{25} + S_7$$

$$S_{17} = C_1 C_{24} + C_{14} C_{25} + S_8$$

$$S_{18} = C_1 C_{25} + S_9$$

$$D_6 = K_7 C_{23} + K_8 C_{24} + K_9 C_{25} + D_3 + K_{12}$$

3. Substituting Variables into Section III

a. Horizontal Deflection

From Equation (7)

$$\delta_{HO} = \delta_{VB} + C_{26} \theta_B + C_{27} P_{HO} + C_{28} P_{VO} + C_{29} M_0 + K_{13} P$$

where

$$C_{26} = R (1 - \cos \beta)$$

$$C_{27} = -\frac{R^3}{EI} \left(\frac{3}{2} \beta - 2 \sin \beta + \frac{1}{4} \sin 2\beta \right)$$

$$C_{28} = \frac{R^3}{EI} \left(\frac{3}{4} - \cos \beta + \frac{1}{4} \cos 2\beta \right)$$

$$C_{29} = \frac{R^2}{EI} (\beta - \sin \beta)$$

$$K_{13} = \frac{\gamma R^4}{EI} \left(\frac{3}{2} \beta - 2 \sin \beta + \frac{1}{4} \sin 2\beta \right)$$

$$\begin{aligned} \delta_{HO} &= S_{10} P_{HO} + S_{11} P_{VO} + S_{12} M_O + D_4 p + C_{26} (S_{16} P_{HO} + S_{17} P_{VO} \\ &\quad + S_{18} M_O + D_6 p) + C_{27} P_{HO} + C_{28} P_{VO} + C_{29} M_O + K_{13} p \\ &= S_{19} P_{HO} + S_{20} P_{VO} + S_{21} M_O + D_7 \end{aligned} \quad (22)$$

where

$$S_{19} = C_{27} + S_{10} + C_{26} S_{16}$$

$$S_{20} = C_{28} + S_{11} + C_{26} S_{17}$$

$$S_{21} = C_{29} + S_{12} + C_{26} S_{18}$$

$$D_7 = D_4 + C_{26} D_6 + K_{13} p$$

b. Vertical Deflection

From Equation (8)

$$\delta_{VO} = \delta_{VB} + C_{30} \theta_B + C_{31} P_{HO} + C_{32} P_{VO} + C_{33} M_O + K_{14} p$$

where

$$C_{30} = R \sin \beta$$

$$C_{31} = -\frac{R^3}{EI} \left(\frac{3}{4} - \cos \beta + \frac{1}{4} \cos 2\beta \right)$$

$$C_{32} = \frac{R^3}{EI} \left(\frac{\beta}{2} - \frac{1}{4} \sin 2\beta \right)$$

$$C_{33} = \frac{R^2}{EI} (1 - \cos \beta)$$

$$\begin{aligned}
 K_{14} &= \frac{\gamma R^4}{EI} \left(\frac{3}{4} - \cos \beta + \frac{1}{4} \cos 2\beta \right) \\
 \delta_{VO} &= S_{13} P_{HO} + S_{14} P_{VO} + S_{15} M_O + D_5 p + C_{30} (S_{16} P_{HO} + S_{17} P_{VO} \\
 &\quad + S_{18} M_O + D_6 p) + C_{31} P_{HO} + C_{32} P_{VO} + C_{33} M_O + K_{14} p \\
 &= S_{22} P_{HO} + S_{23} P_{VO} + S_{24} M_O + D_8 p \quad (23)
 \end{aligned}$$

where

$$\begin{aligned}
 S_{22} &= C_{31} + S_{13} + C_{30} S_{16} \\
 S_{23} &= C_{32} + S_{14} + C_{30} S_{17} \\
 S_{24} &= C_{33} + S_{15} + C_{30} S_{18} \\
 D_8 &= D_5 + C_{30} D_6 + K_{14}
 \end{aligned}$$

c. Rotation

From Equation (9)

$$\theta_O = \theta_B + C_{34} P_{HO} + C_{35} P_{VO} + C_{36} M_O + K_{15} p$$

where

$$C_{34} = - \frac{R^2}{EI} (\beta - \sin \beta)$$

$$C_{35} = \frac{R^2}{EI} (1 - \cos \beta)$$

$$C_{36} = \frac{R\beta}{EI}$$

$$K_{15} = \frac{\gamma R^3}{EI} (\beta - \sin \beta)$$

$$\begin{aligned}
 \theta_O &= S_{16} P_{HO} + S_{17} P_{VO} + S_{18} M_O + D_6 p + C_{34} P_{HO} + C_{35} P_{VO} \\
 &\quad + C_{36} M_O + K_{15} p \\
 &= S_{25} P_{HO} + S_{26} P_{VO} + S_{27} M_O + D_9 p \quad (24)
 \end{aligned}$$

where

$$S_{25} = C_{34} + S_{16}$$

$$S_{26} = C_{35} + S_{17}$$

$$S_{27} = C_{36} + S_{18}$$

$$D_9 = K_{15} + D_6$$

4. Solving for P_{HO} , P_{VO} , and M_O

The loads P_{HO} , M_O , and P_{VO} or δ_{VO} are determined by solving Equations (22), (23), and (24) simultaneously utilizing the known pressure, horizontal deflection, zero rotation, and vertical deflection or P_{VO}

$$S_{19}P_{HO} + S_{20}P_{VO} + S_{21}M_O + D_7p - \delta_{HO} = 0 \quad (22)$$

$$S_{22}P_{HO} + S_{23}P_{VO} + S_{24}M_O + D_8p - \delta_{VO} = 0 \quad (23)$$

$$S_{25}P_{HO} + S_{26}P_{VO} + S_{27}M_O + D_9p = 0 \quad (24)$$

E. MAGNITUDE OF δ_{HO}

The horizontal deflection that a corrugation must undergo is dependent upon three factors: filament wound case pressure strain; relative thermal strain of liner and case; and orientation of corrugation with respect to the case longitudinal axis.

Considering Figure A-2, the deflection δ_{HO} , within the corrugation, must equal 1/2 the total deflection between adjacent corrugations,

$$\delta_{HO} = \frac{W}{2} \left[\epsilon_C + (\alpha_L - \alpha_C) \Delta T - \epsilon_\omega \right]$$

where

$$\epsilon_C = \text{case strain caused by pressure (in./in.)}$$

$$\epsilon_\omega = \text{case shrinkage caused by filament winding tension (in./in.)}$$

α_L = thermal coefficient of expansion of the liner (in./in./°F)

α_C = thermal coefficient of expansion of the case (in./in./°F)

ΔT = total change in temperature from R.T. (°F)

It must be noted here that the length, W , used must be the maximum length between corrugations and that the cross section through this length may yield elliptical corrugation rather than circular. It is therefore necessary to use approximate values of R and B to simulate this factor, which results from changing orientation.

F. STRESSES

The stress considered within the corrugation is the total axial stress resulting from the combined horizontal, and vertical loads and bending moment.

1. At "O"

$$\sigma_O = \frac{P_{HO}}{t} \pm \frac{6M_O}{t^2}$$

2. At "B"

$$\sigma_B = \frac{P_{HB} \sin \beta + P_{VB} \cos \beta}{t} \pm \frac{6M_B}{t^2}$$

and P_{HB} , P_{VB} , and M_B are obtained from Equations (16), (17), and (18), respectively.

3. At "A"

$$\sigma_A = \frac{P_{HA} \sin \beta + P_{VA} \cos \beta}{t} \pm \frac{6M_A}{t^2}$$

and P_{HA} , P_{VA} , and M_A are obtained from Equations (10), (11), and (12).

4. At the Base of Section I

$$\sigma = \frac{P_H}{t} \pm \frac{M}{t^2}$$

where

$$P_H = P_{HA} - C_{13} p$$

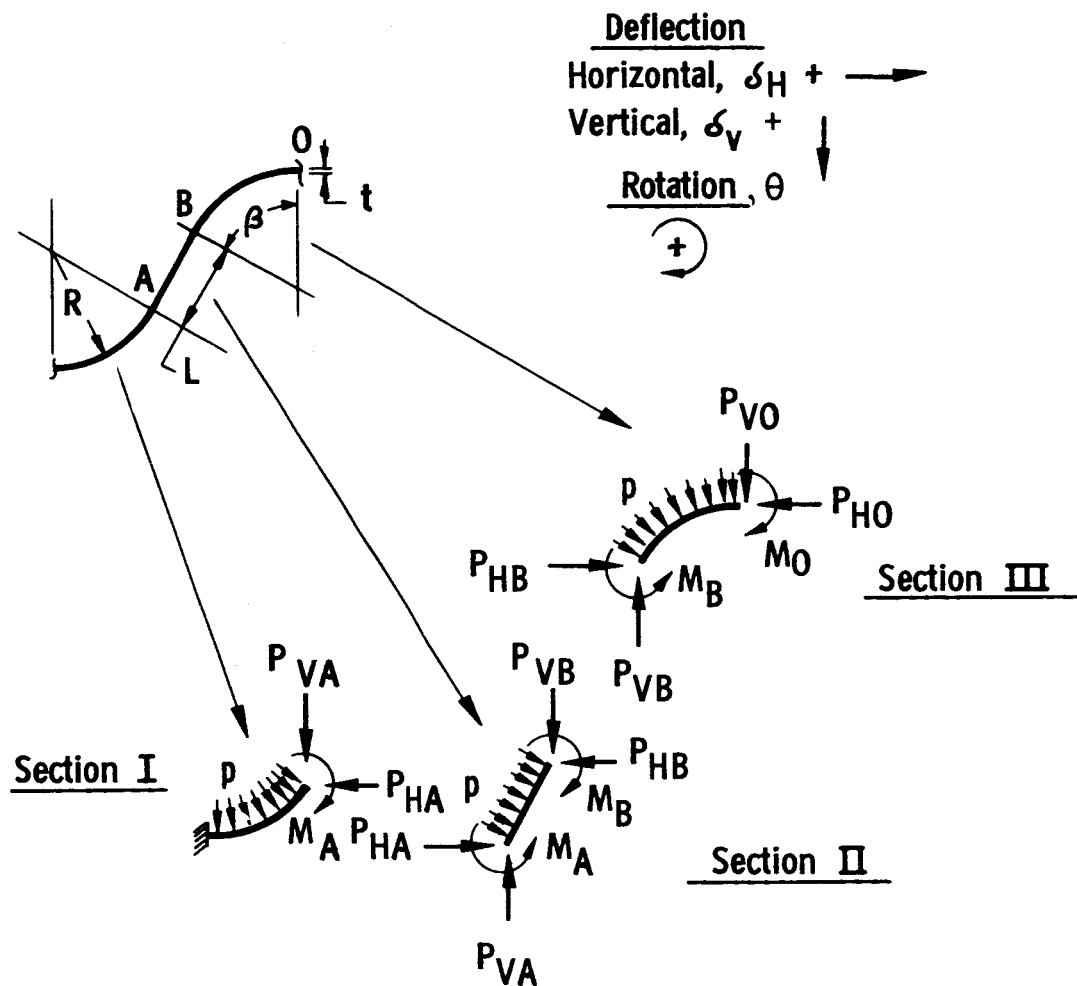
$$M = M_B + C_{13} P_{HA} + C_{14} P_{VA} + K_9 p$$

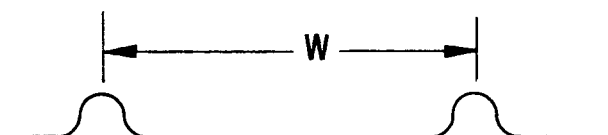
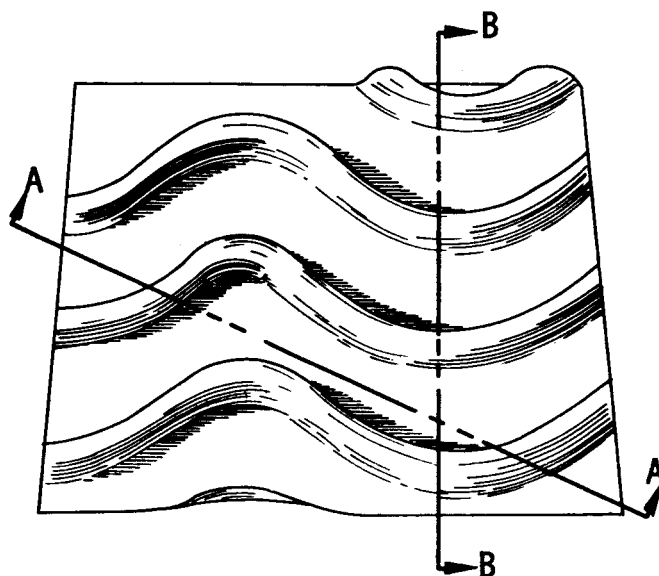
TABLE A-1
CORRUGATION GEOMETRY VARIABLES*

Condition	Material			
	Steel		Aluminum	
	Unsupported	Supported	Unsupported	Supported
R, in.	0.008, 0.012, 0.016, 0.020	0.032, 0.0625, 0.125, 0.25	0.008, 0.012, 0.016, 0.020	0.032, 0.0625, 0.125, 0.25
β , °	30, 45, 60, 75, 90	30, 45, 60, 75, 90	30, 45, 60, 75, 90	30, 45, 60, 75, 90
t, in.	0.002, 0.003, 0.005	0.002, 0.003, 0.005	0.002, 0.003, 0.005	0.007, 0.003, 0.005
L, in.	0	0	0	0
P, psi	175	175	175	175
E, psi	30×10^6	30×10^6	10×10^6	10×10^6
ξ_C , in./in.	0, 0.025	0, 0.025	0.025	0, 0.025

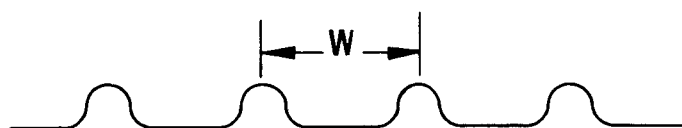
*For each condition all combinations of variables have been evaluated.

** ξ_C is case pressure strain, with stress levels for two values of strain known stress for any required strain may be calculated.





Section A - A rotated 25°



Section B - B rotated 90°

TYPICAL CORRUGATION-PATTERN LENGTH DEFINITION